Radar-aided understanding of semiarid areas: Maximum depression storage and storm motion

García-Pintado J., Barbera G., Erena M., Lopez J.A., Castillo V.M., Cabezas F.

in

Radar-aided understanding of semiarid areas: Maximum depression storage and storm motion

J. García-Pintado*, G.G. Barberá**, M. Erena***, J.A. Lopez***,
V.M. Castillo** and F. Cabezas*

*Euromediterranean Water Institute, Campus de Espinardo, E-30100 Murcia (Spain)
**CSIC-CEBAS, Soil and Water Conservation Department
Campus de Espinardo, PO BOX 164, E-30100 Murcia (Spain)
***Institute of Environmental and Agricultural Development (IMIDA)
C/ Mayor s/n, E-30150 La Alberca, Murcia (Spain)

Abstract. Weather radar supports the estimation of accurate spatiotemporal rainfall inputs. These may be of great help to hone water management strategies, as those involving irrigation plans or flood risk analyses. If these strategies are supported by simulation models, the radar-based estimates should lead in turn to lower biases in estimates of model parameters and to improved model structures. E.g., flash floods pose a danger for life and property and, in semiarid agricultural areas, have a strong relationship with soil loss processes. Unfortunately, in arid and semiarid environment the runoff generation shows a complex nonlinear behavior with a strong spatiotemporal non-uniformity. Predictions by forecasting models are subject to great uncertainty and better descriptions of physical processes at the watershed scale need to be included into the operational modelling tools. We analyze a convective storm, in a 556 km^2 semiarid Mediterranean watershed, with a complex multi-peak response. Radar was instrumental in the understanding and analysis of runoff generation. In the central area, a significant time-variability in the maximum depression storage resulted in the *a posteriori* model structure, pointing to failures in agricultural terraces and/or protection structures. Sensitivity analysis to storm motion indicates that a partial coverage upstream-moving storm on the infiltrating plane results in greater responses.

Keywords. Agricultural land – Semiarid zones – Floods – Hydrological model – Model structure.

Compréhension des zones semi-arides à l'aide de radars : capacité maximale de stockage d'eau dans le micro-relief et mouvement des tempêtes

Résumé. Les radars utilisés à des fins météorologiques contribuent à estimer avec plus d'exactitude l'apport spatiotemporel des précipitations. Ceci peut être d'une grande utilité pour améliorer les stratégies de gestion de l'eau, notamment celles qui font appel à la planification de l'irrigation ou à l'analyse des risques d'inondation. Lorsque ces stratégies s'appuient sur des modèles de simulation, les estimations faites à l'aide de radars devraient permettre à leur tour de réduire les biais que présentent les estimations des paramètres du modèle et d'améliorer les structures du modèle. Par exemple, les crues subites posent un danger pour la vie et la propriété et, dans les milieux agricoles semi-arides, elles sont fortement corrélées aux processus de perte de sol. Malheureusement, dans les environnements arides et semi-arides, le ruissellement provoqué montre un comportement non linéaire complexe et fortement non uniforme spatiotemporellement. Les prédictions des modèles de prévision sont soumises à une grande incertitude et il est donc nécessaire d'incorporer de meilleures descriptions des processus physiques à l'échelle du bassin dans les outils opérationnels de modélisation. Nous analysons une tempête convective, dans un bassin hydrographique méditerranéen semi-aride de 556 km2, présentant une réponse complexe multi-pics. Le radar a fortement contribué à la compréhension et à l'analyse du ruissellement provoqué. Dans la zone centrale, il y a eu une variabilité temporelle significative de la capacité maximale de stockage dans le micro-relief, ce qui a permis de structurer le modèle a posteriori et a révélé les faiblesses des terrasses agricoles et/ou des structures de protection. Une analyse de sensibilité par rapport au mouvement de la tempête a montré que l'on pouvait obtenir de meilleures réponses en se focalisant partiellement en amont du mouvement de la tempête sur le plan d'infiltration.

***Mots-clés.** Terres agricoles – Zones semi-arides – Inondations – Modèle hydrologique – Structure du modèle.*

Options Méditerranéennes, *B no. 67, 2012 – The use of remote sensing and geographic information systems for irrigation management in Southwest Europe*

231

I – Introduction

The past several decades have seen increasing interest in the river systems that drain the world's extensive hyper-arid, arid, semiarid and dry sub-humid regions. These *drylands* cover nearly 50% of the world and support ~20% of its population (Middleton and Thomas, 1997). The spatial generation of runoff is strongly non-uniform in semiarid areas, and is mainly controlled by the rainfall characteristics and the surface physical and chemical properties (Yair and Klein, 1973). Combined effects of tillage patterns with topographic relief in agricultural areas involve a wide range of surface depression storage (Guzha, 2004). At larger scales than the micro-topography, small earth dams in agricultural plots and terraces are generally built in or near drainage lines with the primary purpose for impounding water for storage. These retention structures can inter-cept important amounts of water in areas greater than thousands of square meters, and, after an uncertain retention time, they may eventually fail with hardly foreseeable effects on downstream flows. Although these micro-dams have a high influence on the hillslope hydrology, literature about their behavior is scarce (Bellin *et al.*, 2009).

Uncertainty in model structure is attracting increasing attention in hydrology (Refsgaard *et al.*, 2006), and the presence of time-varying parameters (TVPs) indicates model's structural inadequa-cies (e.g. Lin and Beck, 2007). Maximum depression storage (D) is commonly assumed to remain constant along time in flash flood modelling. Here we allow it to evolve. Its state-dependence is for-mulated by a simple parsimonious model. The *a priori* model structure (constant D) is evaluated versus an *a posteriori* structure with TVP D formulation. We adhere to Knighton and Nanson (2001), who advocate an event-based approach to dryland river hydrology to account for the specific char-acteristics of diverse floods. Thus we analyze in detail one convective storm, in October 2003, in the *Rambla del Albujón* watershed; a semiarid Mediterranean coastal watershed in SE Spain with some urbanized areas and high agricultural pressures. We show how the model is able to locate areas where failures in agricultural protection structures is more likely to have occurred.

We also analyze the sensitivity of the watershed response to storm motion. While this has been the subject of a number of investigations, there is a general lack of analyses conducted on real storms at operational scales, mostly in semiarid environments.

II – Rainfall-runoff modelling framework and analytic techniques

1. Quantitative precipitation estimates (QPE)

QPE errors can dominate the uncertainty in the modeled semiarid runoff, and weather radar has become highly useful for flood forecasting (e.g. Moore, 2002; Carpenter and Georgakakos, 2004). However, radar QPE are prone to inaccuracies, with systematic and random errors often exceeding 100% (Baeck and Smith, 1998). So, adjustment of systematic biases in radar-rainfall using rain gauge measurements has been widely recognized as one of the most important steps in rainfall estimation. Here we used the Concurrent Multiplicative-Additive Objective Analysis Scheme (CMA-OAS) for multi-sensor QPE (García-Pintado *et al.*, 2009a). We used the national radar mosaic, ENS-R-N, from the Spanish Meteorological Agency (AEMET), which includes physically-based processing (with Vertical Profile Reflectivity correction) to estimate reflectivity at the ground level. Ground rainfall data were obtained from 91 tipping-bucket gauges (0.2 mm res-olution), operated by the Agro-climatic Information Service of Murcia region (SIAM), and the Automatic Hydrological Information System (SAIH) of the Segura Basin Hydrological Confederation (CHS). Integration time was 1 h.

2. Modelling framework

We used the MARIAM (Mediterranean and Arid areas Redistribution Input Analysis Model); an event-oriented, distributed, and physically-based forecasting model (García-Pintado *et al.*, 2009b). Inner time step was 1 min, and spatial resolution 50 x 50 m. The *a priori* model structure considers terrain relief as static. Two relief properties were identified as likely time-varying in the observed rainfall-runoff event: maximum depression storage (*D*) in land, and roughness in channels. Here we focus on the former. The following subsection shows how we modeled the observations through a dynamic formulation of *D*. The innovated model structure is such that the physical/conceptual meaning of *D* remains the same as in the *a priori* structure.

3. Dynamic maximum depression storage

The maximum depression storage *D* is a relief-dependent property that indicates the maximum water that could be stored on surface. Available watershed models consider *D* as a constant parameter, either lumped or spatially distributed. Then, either *D* is applied at the beginning of the storm and only water in excess of *D* is allowed to runoff, or the rate of filling of the deposit *D* is inversely proportional to the available remaining space in *D*. Several formulations have been proposed for the latter option; which allows for a proportion of the effective rainfall to be released as runoff, even for small rainfall rates, before *D* is completely full.

Mitchell and Jones (1978) demonstrated the value of a dynamic description of the maximum depression storage at the plot scale. Our focus is, however, on processes occurring at the catchment scale. Values of *D* may remain fairly constant in totally natural, commonly more vegetated, areas. However, our field observations in storm events indicate (i) that anthropogenic "soft structures", mostly for agricultural tasks (such as tilling patterns, terraces, small earth dams around agricultural plots...), may lead to high *D*, and (ii) that intense energy storms and floods weaken the retention capability of these structures, whose eventual failure and possible cascading effect, speeding up downstream flows, is difficult to predict. Sandercock *et al.* (2007) comment that small earth dams around agricultural plots have a big influence on the connectivity of the hill slope; however, during large rainfall events the runoff might cause them to collapse, and at that moment the runoff flow might damage all lower lying earth dams as well. Our view of this process indicates that the global retention capability of agricultural semiarid watersheds fails by structural breaching (gradual failure), with increased hydraulic pressures implying more abrupt breaching.

We suggest a model in which the time history of water stage *h(t)* produces a gradual damage accumulation in the initial *D* (D_0), which may fall up to a final operation mode (D_s), after all the "soft" spatially distributed retention capability of the watershed has failed. Here we propose a time-varying maximum depression storage *D(t)* to be simulated by a logistic decay:

$$D(t) = Ds + \frac{(D_0 - D_s)\,(1 + \alpha_D)}{1 + e^{\beta_D \int_0^t h(\tau)d\tau}} \tag{1}$$

where the parameters α_D (–) and β_D (m^{-1} s^{-1}) control the shape of this S-type decay model, and τ is a dummy variable of time. For a specific (α_D; β_D), relatively low *h(t)* values may never be able to significantly modify the initial *D(t)* value, D_0. However, relatively high *h(t)* values may cause structures to collapse in a very short time. Equation (1) may be combined with the formulations that allow some water stored in *D(t)* to be released as a function of the level *h(t)* (e.g. see Bras, 1990). However, this would require extra parameters. Thus taking into account the principle of parsimony, just water in excess of *D(t)* is allowed here to be routed. In addition, while the possible combinations of the four parameters in equation (1) (D_0, D_s, α_D, β_D) allow a wide spectrum of decaying depression storage evolutions, the constraint $\alpha_D = \beta_D$ was added in this study to further

reduce the analyzed parametric space. Also, this constraint facilitates evaluation of feasible parameter ranges through mapping α_D and β_D onto a parameter with temporal meaning. That is, we can solve equation (1) for a parameter l_D (which equals both α_D and β_D) as a function of a desired $D(t)$ evolution under the hydraulic pressure given by a constant water column h applied a specific time span Δt. So, if for a constant h we consider the half-life $\Delta t_{0.5}$ as that time in which $D(t)=(D_0+D_s)/2$, we can make the corresponding substitutions in equation (1) to obtain:

$$f(\lambda_D) = 1 + \lambda_D \left(2 - e^{\lambda_D h \Delta t_{0.5}}\right) = 0 \tag{2}$$

whose solution will yield the parameter l_D. Then, l_D is used for substituting both α_D and β_D in the theoretical curve, given by equation (1), which will be used in the model with time-varying $h(t)$ conditions. The function $f(l_D)$ in equation (2) has a well defined maximum and only one real root l_D over $[0, \infty)$, and its solution may be found by Newton's method. If, in addition, h is set to $h=(D_0+D_s)/2$ in equation (2), the values of $\Delta t_{0.5}$ represent the half-life of the structures when these are constantly subjected to a hydraulic head equal to the half of the decaying range allowed for maximum depression storage. This approach still allows a wide variety of $D(t)$ behaviors as a function of the free parameters (D_0; D_s, and $\Delta t_{0.5}$) input into the model.

4. Watershed and gauge points

Mean annual precipitation in the *Rambla del Albujón* watershed (556 km^2) is 300 mm, generally concentrated short episodic stormy events. Potential evapotranspiration is 890 mm year^{-1}. Figure 1 shows Hydrological response Unit (HRU; area assumed as responding homogeneously) sub-division and flow gauge points.
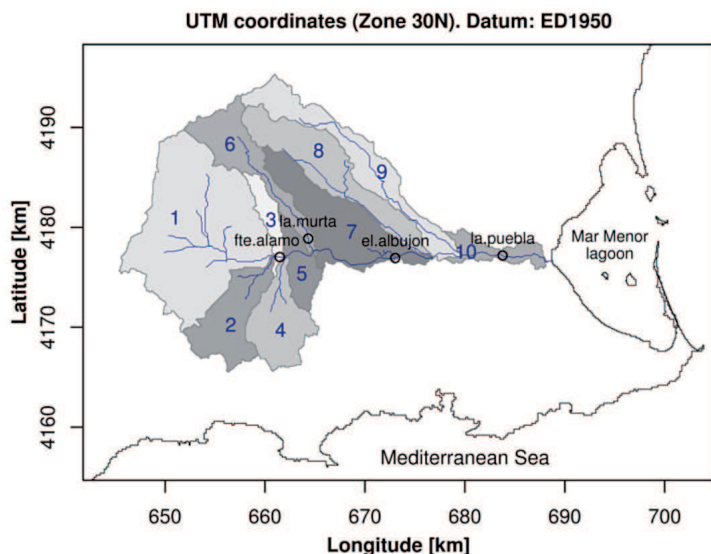

Fig. 1. Location of the Rambla del Albujón watershed and the Mar Menor coastal lagoon at the Southeast of Spain. HRUs are numbered in flow aggregation order. Circles indicate gauge locations.

5. Calibration approach and a priori parameter distribution

We evaluated model and parameter uncertainty with the Generalized Likelihood Uncertainty Estimation (GLUE) methodology (Beven and Binley, 1992). The problem was posed so that the model with constant D is a subset structure of that with time-varying D, in which specific additional parameters in the improved structures take specific values. Evaluation of behavioral runs (those with adequate likelihood) allows making inferences to update our *a priori* beliefs. Evaluation of time-decaying D considers three parameters: D_0; D_s, and $\Delta t_{0.5}$. For every HRU_i, in which maximum depression storage was evaluated as time-decaying, $D_i(t)$, half-life $\Delta t_{0.5}$ was always evaluated with a priori uniform distribution with $\Delta t_{0.5}$ h. On the other hand, we considered that both the initial and the final values of maximum depression storage (D_{0i}, D_{si}) had *a priori* uniform density ranging between the same bounds $[D_{i,\min}, D_{i,\max}]$. The sampled were drawn from these uniform priors. Then, for each j random sample, if $D_{si,j} > D_{0i,j}$, the former was set to the latter value as $D_i(t)$ was just considered to decay. We are interested in the parameter defined by the random variable $\Delta D_i = D_{0i} - D_{si}$, and this experimental design gives equal a priori probability $f = 0.5$ to the hypothesis that $\Delta D_i = 0$, and to the alternative hypothesis that $D_i(t)$ decays. In effect, being $\Delta D_{i,r} = D_{i,\max} - D_{i,\min}$, the resulting prior right-continuous cumulative distribution function ($F(x)=P(X\leq x)$) of ΔD_i, is shown in Figure 3.

Objective functions used for multicriteria analysis are shown in Table 1, where $O = \{o_1,…,o_n\}$ is the vector of streamflow observation data at time steps $1,…, n$, and $S(\xi, \Theta) = \{s_1(\xi, \Theta),…,s_n(\xi, \Theta)\}$ is the vector of simulated flows for a specific structure ξ with a specific parameter set Θ.

Considering the objective functions and gauge points, we refer to a behavioral simulation under a specific OF and considering the observed hydrograph at point X as OF-X-behavioral. If all OF criteria are fulfilled at X, the simulation is denoted as total-X-behavioral, and if all available nested hydrographs fulfill a specific OF criterion, it is a OF-global-behavioral.

Table 1. Objective functions and behavioral bounds considered in this study

OF[†]	Formula	Behavioral
PDIFF[††]	$\|max_{1\leq t\leq n} \{o_t\} - max_{1\leq t\leq n} \{s_t(\xi, \Theta)\}\|/max_{1\leq t\leq n} \{o_t\}$	[0.4-0]
PTLAG[††,†††]	$\|time\{max_{1\leq t\leq n} \{o_t\}\} - time\{max_{1\leq t\leq n} \{s_t(\xi, \Theta)\}\}\|$	[3600-0]
FV	$\left\|\sum_{t=1}^{n}(o_t - s_t(\xi,\Theta))\right\| / \sum_{t=1}^{n} o_t$	[0.2-0]
NS	$1-\sum_{t=1}^{n}(o_t - s_t(\xi,\Theta))^2 / \sum_{t=1}^{n} (o_t - \overline{o})^2$	[0.4-1.0]

[†] PDIFF: absolute normalized peak difference; PTLAG: absolute time lag for peaks; FV: absolute normalized volume difference; NS: Nash-Sutcliffe efficiency; see text for definition of terms in formulae.

[††] Just the global peak is considered for these statistics.

[†††] (s); remaining OF are dimensionless.

III – Calibration results and discussion

Calibration was conducted in three stages: Stages I and II have a lumped and a distributed parameterization, respectively, for the a priori model; and Stage III analyzes the posterior model structure (dynamic D). Here we focus on D. Remaining parameters (e.g. hydraulic conductivity or friction coefficients) were sampled, for all stages, from common *a priori* distribution and ranges.

Stage I, with lumped parametrizations, completely failed in simulated the watershed hydrology and obtaining the multi-peak observed response. Stage II, with spatially distributed parameter, beha-

ved much better in simulating the different behaviour of the various parts of the watershed. However, still a systematic bias evidenced that a certain amount of water should be first retained in the central parts of the watershed, and it should be later released, in a relatively abrupt way, to contribute to the second flow wave coming from the upper parts of the watershed. This problem was resolved in Stage III, with specific accounting of this process through the time-varying maximum surface depression storage. Figure 2 shows some simulation results from Stage III.
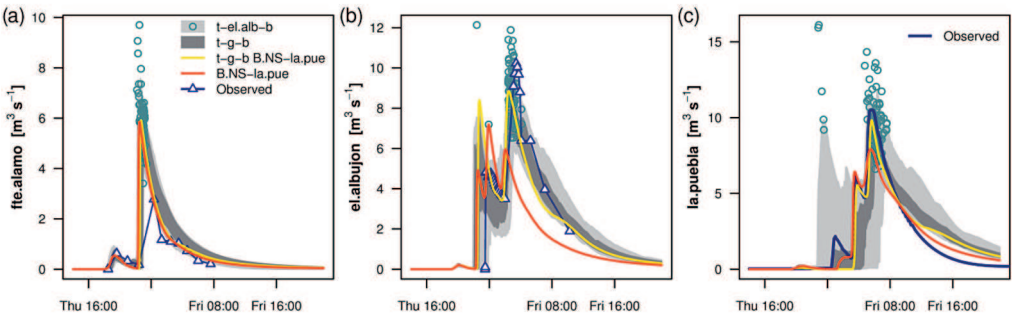

Fig. 2. **Stage III. Step 2. MC simulation (21 000 runs). Light grey areas cover the GLUE-sense 95% confidence intervals (c.i.) of total-el.albujon-behavioral simulated hydrographs (t-el.alb-b, n = 94) at (a) fte.alamo, (b) el.albujon, and (c) la.puebla. Dark grey areas cover the 95% c.i. of total-global-behavioral simulations (t-g-b, n = 37). The t-g-b simulation with the highest NS at la.puebla (NS = 0:84) is in yellow, and the best NS-la.puebla simulation (NS = 0:90, but not in the t-el.alb-b subset) is in red.**
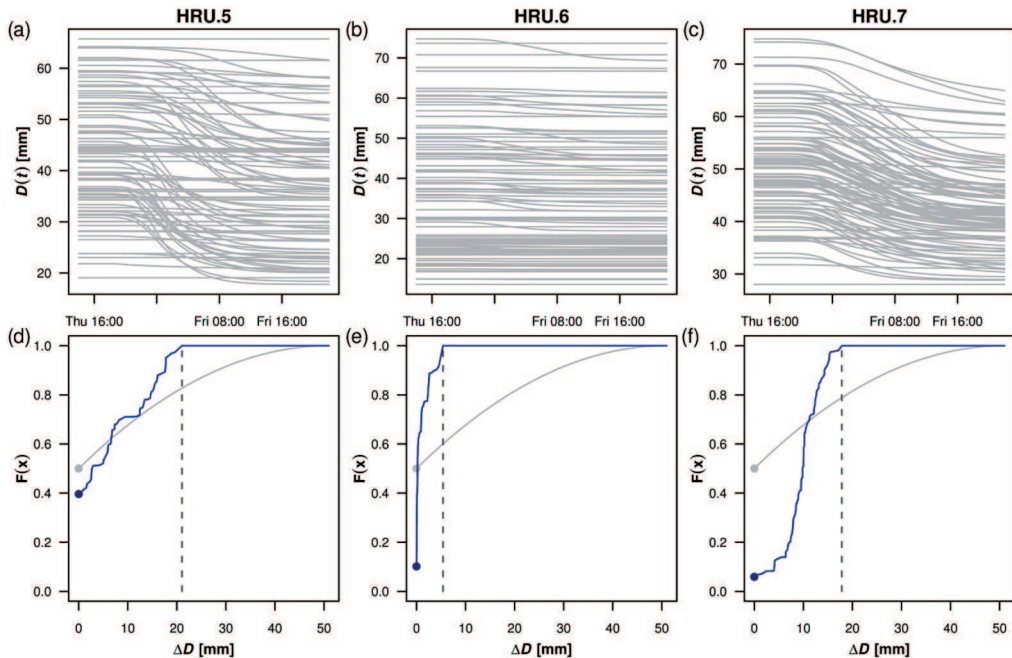

Fig. 3. **Stage III. Simulations that were simultaneously total-fte.alamo-behavioral and total-el.albujon-behavioral, showing areal mean $D(t)$ evolution in the HRUs contributing to runoff between these two measurement points and evaluated for time-varying maximum depression storage. The bottom row show corresponding a priori (grey) and a posteriori (blue) cumulative distribution functions of ΔD.**

GLUE-based inference supported the hypothesis that the structural breaching was into effect, leading to dynamic maximum depression storage. The magnitude of the time-variability of the maximum depression storage had a high spatial variability. Figure 3 indicates that the posterior distribution of ΔD in HRU.7 gave a very small probability mass (P(X = 0) = 0.07) to the hypothesis that $\Delta D = 0$, and most of the probability concentrated around $\Delta DHRU.7 = 10$ mm. In HRU.5 there was no clear support to the alternative hypothesis, but the behavioral range was limited up to $\Delta DHRU.5 = 22$ mm. In HRU.6, was relatively disproved (P(X = 0) = 0.2); however, the behavioral probability range, $\Delta DHRU.6$ [0, 5] mm, indicated more stable retention structures with respect to HRU.7. As a comparison, Bellin *et al.* (2009) found in a nearby catchment that a storm with a return period of 8 years produced structural damages in 16% of walls and other soil conservation structures.

IV – Sensitivity of simulated response to storm motion

The importance of storm motion on the hydrograph shape has been acknowledged, but related literature is scarce. The October 2003 storm was aligned with the main channel. Thus the radar-based QPE is an opportunity to conduct a concise simulation analysis about the hypothetical scenario of an identical storm with reversed upstream motion. We simulated the watershed response to the upstream storm motion with the ensemble of parameter sets within NS-el.albujon-behavioral or NS-la.puebla-behavioral simulations in the posterior model (3415 sets). Figure 4 shows three dimensionless descriptors of the integrated hydrograph at la.puebla. These are (a) relative flow volume (RFV [–]), i.e., ratio between total simulated flow and total observed flow with the downstream motion; (b) relative peak flow (RPF [–]), i.e., ratio between peak simulated flow and peak observed flow; and (c) relative Shannon entropy (RSE [–]) as a descriptor of the general compression or dispersion of the hydrograph regardless of the net flow amounts. To calculate RSE, first the hydrographs were scaled to integrate to one (as a PDF); then, RSE was obtained as the ratio of the Shannon entropy (Shannon, 1948) obtained for the scaled hydrograph to that obtained for a uniform distribution function. Thus RSE [0, 1], where higher values indicate higher dispersion.

Hydrographs were significantly affected by the storm movement, and global behavior may be summarized in three features. First, the storm moving upstream had a trend to decouple the successive peaks of the hydrograph obtained in the downstream-moving storm. Thus the runoff wave generated in HRU.1 arrived generally later than that generated in the middle areas as to form a more independent second flow wave at the outlet with respect to that resulting from the downstream-moving storm. So, the flow tended to be more distributed in time resulting in higher RSE values (Fig. 4). Second, despite this partial decoupling, the individual runoff amounts and peaks of the upstream-moving storm hydrograph pertaining to either water generated in the middle areas or water coming from HRU.1 tended to be greater than those for the downstream-moving storm. As a result, the total runoff at la.puebla was quasi-systematically higher for the former (RFV in Fig. 4). Some past studies, considering impervious surfaces, concluded that downstream-moving storms tend to create higher peaks (e.g. Ogden *et al.*, 1995; Singh, 2002). However, Singh (2005), with a kinematic analytical solution for runoff resulting from storms with partial coverage moving on an infiltrating plane, drew the conclusion that "for the same areal coverage and the same duration of storm, the peak is greater for the storm moving upstream than that for the storm moving downstream". This is supported by our results, and the most likely reason being that infiltration has higher opportunity time to occur for storms moving downstream. Third, despite the individual peaks of the upper and middle areas of the watershed increased for the upstream-moving storm, its decoupling implied that these peaks did not overlap as much as they did in the downstream-moving storm. As a result, the absolute peaks were approximately similar in both scenarios, with just slight increases for the upstream-moving storm (RPF in Fig. 4).
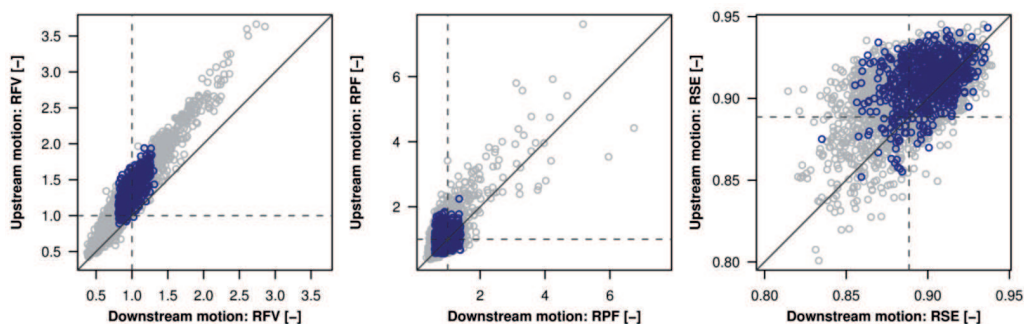
Fig. 4. Effect of storm motion on the watershed response. Dark blue indicates total-la.puebla-behavioral simulations. Dashed lines refer to the observed hydrograph.

V – Conclusions

We show a time-varying formulation for maximum depression storage, whose evolution was significant in the central areas of a semiarid watershed during a flash flood driven by a convective storm. Radar information was instrumental in understanding the runoff generation mechanisms and in the estimation of the *a posteriori* model structure. Radar data also supported the evaluation of storm motion, for which our results show that, in the evaluated case, a storm with partial coverage moving upstream on the infiltrating plane tends to create greater responses. A relationship with failures in agricultural terraces and other soil protection structures was identified.

Acknowledgments

References

Baeck M.L. and Smith J.A., 1998. Rainfall estimation by the WSR-88D for heavy rainfall events. In: *Weather Forecast*, 13, p. 416-436.

Beven K.J. and Binley A.M., 1992. The future of distributed models: model calibration and uncertainty prediction. In: *Hydrol. Proc.*, 6, p. 279-298.

Bellin N., van Wesemael B., Meerkek, A., Vanacker, V. and Barberá, G.G., 2009. The decay of soil and water conservation structures. A case study from Southeast Spain. In: *Catena*, 76, p. 114-121.

Carpenter T.M. and Georgakakos, K.P., 2004. Impacts of parametric and radar rainfall uncertainty on the ensemble streamflow simulations of a distributed hydrologic model. In: *J. Hydrol.*, 298, p. 202-221.

García-Pintado J., Barberá G.G., Erena M. and Castillo, V.M., 2009a. Rainfall estimation by raingauge-radar combination: a concurrent multiplicative-additive approach. In: *Water Resour. Res.*, 45, W01415. doi:10.1029/2008WR007011.

García-Pintado J., Barberá G.G., Erena M. and Castillo, V.M., 2009b. Calibration of structure in a distributed forecasting model for a semiarid flash flood: dynamic surface storage and channel roughness. In: *J Hydrol,* 377, p. 165-184.

Guzha A.C., 2004. Effects of tillage on soil microrelief, surface depression storage and soil water storage. In: *Soil Tillage Res.*, 76(2), p. 105-114.

Knighton A.D. and Nanson G.C., 2001. An event based approach to the hydrology of arid zone rivers in the Channel Country of Australia. In: *J. Hydrol.*, 254(1-4), p. 102-123.

Lin, Z. and Beck, M.B., 2007. On the identification of model structure in hydrological and environmental systems. In: *Water Resour. Res.* 43, W02402. doi:10.1029/2005WR004796.

Middleton N.J. and Thomas D.S.G., 1997. *World Atlas of Desertification*, second ed. UNEP/Edward Arnold, London.

Mitchell J.K. and Jones Jr. B.A., 1978. Micro-relief surface depression storage: changes during rainfall events and their application to rainfall–runoff models. In: *J. Am. Water Resour. Assoc.*, 14(4), p. 777-802.

Moore R.J., 2002. Aspects of uncertainty, reliability and risk in flood forecasting systems incorporating weather radar. In: *Risk, Reliability, Uncertainty and Robustness of Water Resources Systems* (ed. By J. J. Bogardi and Z. W. Kundzewicz). Cambridge University Press, pp. 30-40.

Ogden F.L., Richardson J.R. and Julien P.Y., 1995. Similarity in catchment response: 2. Moving rainstorms. In: *Water Resour. Res.*, 31(6), p. 1543-1547.

Refsgaard J.C., van der Sluijs J.P., Brown J. and van der Keur P., 2006. A framework for dealing with uncertainty due to model structure error. In: *Adv. Water Resour.*, 29, p. 1586-1597. doi:10.1016/j.advwatres.2005.11.013.

Sandercock P.J., Hooke J.M., Lesschen J.P. and Cammeraat L.H., 2007. Sediment connectivity. In: *Conditions for Restoration and Mitigation of Desertified Areas Using Vegetation (RECONDES): Review of Literature and Present Knowledge* (ed. by European Commission, Directorate-General for research Information and Communication Unit). ISBN: 92-79-03072-8.

Shannon C.E., 1948. A mathematical theory of communication. In: *Bell Syst. Tech. J.*, 27, p. 379-423, 623-656.

Singh V.P., 2002. Effect of the duration and direction of storm movement on planar flow with full and partial areal coverage. In: *Hydrol. Proc.*, 16, p. 3437-3466.

Singh V.P., 2005. Effects of storm direction and duration on infiltrating planar flow with partial coverage. In: *Hydrol. Proc.*, 19, p. 969-992.

Yair A. and Klein M., 1973. The influence of surface properties on flow and erosion processes on debris covered slopes in an arid area. In: *Catena*, 1, p. 1-18.